infrastructures

MDPI

Article

Parametric Investigation of Interaction between Soil-Surface Structure and Twin Tunnel Excavation: A Comprehensive 2D Numerical Study

Ammar Alnmr [1,*], Ashraf Sheble [2], Richard Ray [1] and Hussein Ahmad [2]

[1] Department of Structural and Geotechnical Engineering, Széchenyi István University, 9026 Győr, Hungary; ray@sze.hu

[2] Department of Geotechnical Engineering, Tishreen University, Latakia P.O. Box 2230, Syria; ashraf.sheble@tishreen.edu.sy (A.S.); hussein.ahmad@tishreen.edu.sy (H.A.)

* Correspondence: alnmr.ammar@hallgato.sze.hu

Abstract: The growing demand for transportation tunnels in densely populated urban areas has led to the widespread adoption of twin tunnel configurations in contemporary infrastructure projects. This research focuses on investigating the complex interaction between soil, structures, and the excavation of twin tunnels. The study employs the tunnel boring machine (TBM) method and utilizes two-dimensional numerical modeling based on the finite element method (FEM). The numerical model is validated by comparing its results with field measurements obtained from a twin tunnel project in Italy, specifically the New Milan Metro Line 5. A comprehensive parametric study is conducted to analyze various parameters that influence soil–structure interaction during tunnel excavation. These parameters include the positioning of the tunnels in relation to each other, the spacing between them, the presence of structures above the tunnels, eccentricity between the structure axis and tunnel axis, and tunnel depth and diameter. Moreover, a comparative analysis is performed between scenarios with and without structures to elucidate the impact of structure presence on the interaction phenomenon. The research findings provide valuable insights into the intricate behavior of twin tunnels and their interaction with the surrounding soil and structures.

Keywords: twin tunnel; soil-structure interaction; 2D numerical study; tunneling

check for updates

Citation: Alnmr, A.; Sheble, A.; Ray, R.; Ahmad, H. Parametric Investigation of Interaction between Soil-Surface Structure and Twin Tunnel Excavation: A Comprehensive 2D Numerical Study. *Infrastructures* **2023**, *8*, 124. https://doi.org/10.3390/infrastructures8080124

Academic Editor: Francesca Dezi

Received: 2 June 2023
Revised: 5 August 2023
Accepted: 9 August 2023
Published: 11 August 2023

1. Introduction

Cities are currently grappling with pressing transportation and communication challenges, as well as significant traffic congestion in their central areas. As a result, city residents are considering the utilization of underground spaces by excavating metro and transportation tunnels. A prevailing approach involves the establishment of multiple adjacent tunnels (typically two or three) to optimize the utilization of subterranean areas beneath cities. However, tunnel excavation induces soil deformations in the surrounding area, which propagate towards the surface, resulting in the formation of subsidence troughs in non-built-up regions. Conversely, when a structure is present above the tunnel, a complex interaction arises among the soil, tunnel, and structure. This interaction plays a crucial role in influencing the settlement phenomena associated with tunnel excavation. Furthermore, the interaction between the excavation of twin tunnels during construction poses an additional consideration that warrants careful examination.

Several studies have investigated the effects of excavating twin tunnels on surrounding structures. Gong et al. [1] conducted a numerical study on a historical masonry building in Shanghai, assessing the deformations resulting from the excavation. Similarly, Kaczmarek et al. [2] performed a 2D numerical study in Warsaw, focusing on the impact on adjacent infrastructure such as buildings and slopes. Peng et al. [3] examined the effect of tunnel excavation on adjacent masonry buildings by combining field measurements from the

Zhengzhou Metro Line 5 with numerical analysis. They evaluated surface subsidence, subsidence, and deformation in the masonry structures.

In addition, Mathew et al. [4] conducted measurements and numerical analysis to investigate the influence of soil stratification on the interaction between soil, structures, and the excavation of twin tunnels. Hao et al. [5] conducted a numerical study based on field measurements during the excavation of the Qingduo Metro Line 1, focusing on the impact on an existing masonry building. Fargnoli et al. [6] addressed the interaction between twin tunnels in both green field conditions and with the presence of a structure. They compared numerical modeling results with measurements obtained during the excavation of the New Milan Metro Line 5. Milan Metro Line 5 was selected as a significant case study because of the availability of extensive field measurements. These measurements played a crucial role in calibrating the numerical model used in this study, ensuring its accuracy and reliability in simulating twin tunnel interactions.

Numerous researchers have conducted parametric studies to investigate the interaction between soil, tunneling, and surface structures. Maleki [7] examined the effects of structure stiffness, weight, width, and eccentricity between the tunnel and structure axes, taking into account the surface placement of the structure. Katebi [8] focused on tunnel depth, structure width, weight, and eccentricity, studying their impact on internal forces and deformations of the tunnel lining. Giardina [9] conducted a numerical study based on Farrell's centrifuge test [10] to explore the influence of structure stiffness, weight, and volume loss. Son [11,12] conducted numerical studies on brick buildings situated on sandy and clay soils, investigating settlement variations caused by different volume loss, tunnel depth, and diameter. Boldini [13] investigated the influence of structure characteristics, including the number of stories and weight. In the context of tunnel positioning, Shahrour et al. [14] conducted a two-dimensional numerical study that examined the effect of the relative placement of two tunnels in a green field condition. Their investigation focused on analyzing the influence of the positioning of the two tunnels in relation to each other. Mirhabibi et al. [15] specifically addressed the case of two tunnels in the context of the Shiraz Metro Line 1 through a two-dimensional numerical study. They conducted a parametric analysis considering numerous factors, such as the depth of the tunnels and the spacing between them, particularly when the structure is symmetrically placed with respect to the tunnel axis. This symmetric configuration represents the least hazardous case, minimizing the difference in subsidence between the two ends of the structure. Additionally, the study explored the impact of the distance between two symmetrical structures relative to the tunnel axis, the weight of the structure, and the presence of one or two structures located above the tunnels. In recent years, various numerical and analytical studies have been conducted to explore the impact of twin tunnel excavations on surrounding structures and soil [16–22]. For instance, Duangsano et al. [16] investigated the effect of twin tunnel excavation on structures located on pile foundations in the case of the Bangkok MRT Orange Line. Similarly, Sarfarazi and Asgari [17] focused on the development of collapse surfaces during tunnel excavations for both single tunnel and twin tunnel cases. Moreover, Li et al. [18] conducted a numerical study on the influence of the excavation of a second tunnel on the internal forces of adjacent tunnel segments. Khan et al. [19] developed a miniature laboratory model for twin tunnels and explored the effects of groundwater levels and tunnel distances on settlement. However, their study was limited to the green field scenario without considering the presence of surface structures. Furthermore, Chortis and Kavvadas [20] studied the interaction effect between twin tunnels by analyzing the impact of each tunnel on the internal forces of the other. Cavalcanti et al. [21] compared two-dimensional numerical analysis with semi-empirical methods to calculate subsidence resulting from twin tunnel excavation in green field conditions.

Most of the reviewed studies have focused on investigating the interaction between soil, structures, and the excavation of two tunnels. These studies have primarily compared numerical analysis results with field measurements obtained from constructed projects. However, in terms of parametric studies, the emphasis has primarily been on examining the interaction between soil, structures, and the excavation of a single tunnel, with limited attention given to the specific issue of the interaction resulting from the excavation of twin tunnels. Thus, further research is needed to address this specific aspect of the interaction between twin tunnel excavations.

This study represents an extension of a previous study [23], which primarily focused on the analysis of a single tunnel. In contrast, the current study delves into twin tunnels, enabling a comprehensive understanding of the distinctive interaction effects inherent in this specific tunnel configuration and its impact on surface structures.

The primary objective of this study is to bridge the identified research gap by specifically focusing on the interaction arising from the excavation of twin tunnels. Through a comprehensive parametric analysis, the study aims to delve into the complex interplay between soil, structures, and the excavation of twin tunnels. Specifically, the investigation will consider key factors such as the distance between the axes of the twin tunnels, the diameter of the twin tunnels, the depth of excavation, the eccentricity between the axes of the twin tunnels and the axis of the structure, the spacing between the two ends of two symmetrical structures in relation to the axis of the twin tunnels, and the relative positioning of the two tunnels along their axis. To gain a deeper understanding of this phenomenon, a comparative analysis was performed between the outcomes obtained under green field conditions and those considering the presence of a surface structure.

By thoroughly examining these parameters, the study endeavors to shed light on the intricate interactions associated with twin tunnel excavations. Numerical simulations and analysis will be conducted to elucidate the effects and implications of varying these factors on the behavior of the soil and structures. The findings from this study are anticipated to contribute significantly to the existing knowledge base, providing valuable insights into the interaction mechanisms specific to the excavation of twin tunnels.

2. Milan Twin Tunnel Case Study

The Milan Metro Line 5, a twin tunnel system located in Milan, Italy, spans a distance of 12.6 km and serves as a crucial transportation route with 19 access stations [6]. The focus of this study lies on specific portions of the metro line, namely the 1.3 km stretch between the San Siro and Segesta stations, as well as the approximately 600 m segment between the Lotto and Portello stations. These sections were selected due to their relevance to the research objectives. The investigation centers on the interaction between the twin tunnels and the surrounding ground conditions in the presence of green-field conditions.

The ground section S16 was specifically chosen as a representative example, as it exhibits average values of maximum settlements for the analyzed portion of the metro line. The twin tunnels were partially excavated below the water table, maintaining a distance of 15 m between their axes and achieving a mean depth of 15 m [6]. To minimize ground movements within densely populated areas, earth pressure balance (EPB) machines were employed for excavation. These machines employ a rotating cutter-head, while the excavated material is kept under pressure within the bulk chamber to ensure face stability and restrict surface settlements [6].

The metro line is situated within a granular unit formation, predominantly composed of fluvioglacial and alluvial gravel and sand [6]. During the project's design phase, an extensive geotechnical investigation was conducted along the entire metro line route. This investigation involved core drillings, open pipe piezometers, standard penetration test (SPT) measurements, and constant-head Lenfranc-type permeability tests [6].

Furthermore, the soil stratigraphy encountered at the San Siro–Segesta and Lotto–Portello stations reveals important ground conditions. A hydrostatic water table was detected approximately 15 m below the ground surface level using open-pipe piezometers. The dominant characteristic of the deposit in these areas is gravelly-sand soil, which is generally homogeneous across the investigated segments of the route. However, it should be noted that between the stations of Lotto and Portello, a distinct sandy-silt layer measuring 5 m in thickness was identified at depths ranging from 20 to 25 m.

3. Contraction Method

The contraction method, introduced by Vermeer and Brinkgreve [24], is a numerical technique employed for simulating ground loss during tunneling. This method is distinct from other approaches in that it does not necessitate a highly refined mesh of elements, which is typically required in methods involving a specialized fine mesh between the tunnel shell and shield. As a result, the contraction method has gained widespread adoption in the field of tunneling simulations.

Contraction Method (2D)

The 2D modeling of the contraction method involves two distinct calculation phases aimed at simulating the impact of tunnel excavation, as depicted in Figure 1. The initial phase of the calculation involves deactivating the soil cluster within the tunnel's perimeter, indicating the excavation of the tunnel. The water present within the soil cluster is also removed (cluster dry), and measures are taken to prevent the surrounding groundwater from infiltrating the cluster. Additionally, a tunnel lining is installed to stabilize the tunnel structure. However, an instability arises due to the imbalance between the weight of the tunnel lining and the excavated soil within the tunnel, resulting in uplifting of the tunnel lining.

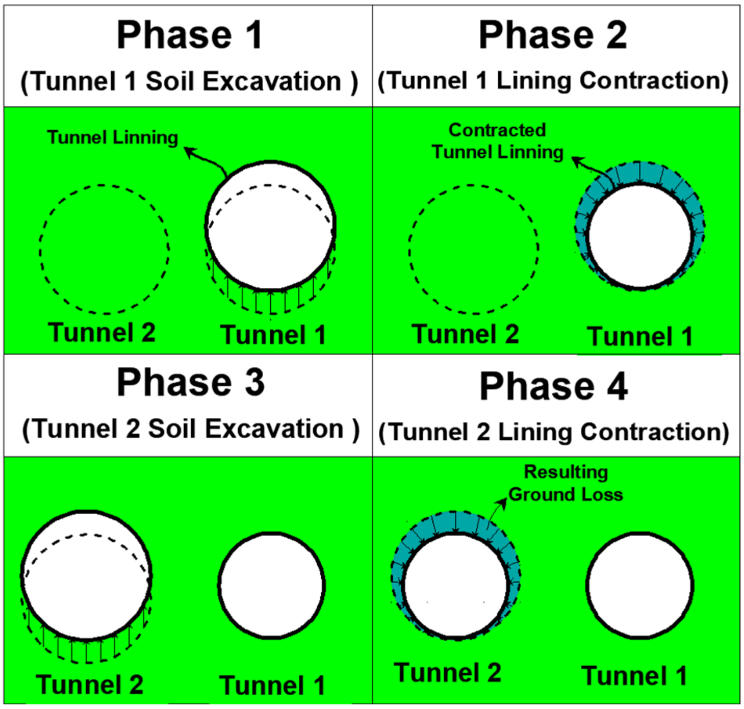

Figure 1. Contraction method (compiled by the authors based on [25]).

In the second phase, the tunnel undergoes a controlled contraction process, gradually reducing the size of the tunnel lining until the prescribed contraction ratio is achieved. The calculation of the contraction ratio is determined using Equation (1) [25]:

$$\text{Contraction} = \frac{(Original\ Tunnel\ Area - Tunnel\ Area\ At\ Current\ Phase)}{Original\ Tunnel\ Area} \tag{1}$$

4. Tunnel Geometry and Site Conditions

To validate the accuracy of numerical analysis and refine the soil behavior, a comprehensive numerical model employing the finite element method was employed to simulate a twin tunnel. The twin tunnel, which was completed in 2013, possesses an outer diameter of 6.7 m. The excavation process employed an earth pressure balance shield (EPB shield) with a length of 9.8 m, relying on continuous front support. This support mechanism resulted in pressure values escalating from 106 kPa at the tunnel crown to 185 kPa at the tunnel base. The twin tunnel's lining comprises precast reinforced concrete rings, referred to as segments, measuring 0.3 m in thickness and 1.4 m in length.

Numerous field measurements were conducted throughout the project, including the monitoring of surface settlements above the twin tunnel under green field conditions during the initial phase of construction (single tunnel) and subsequent phase (twin tunnel) [6]. These measurements provide critical insights into the behavior of the tunnel and its surrounding soil, offering valuable data to analyze and comprehend the occurrence and distribution of surface settlements.

Field measurements were employed as a means of calibrating the numerical model, thereby ensuring its accuracy in capturing the intricate behavior of the twin tunnel. Through a meticulous comparison of the field measurements with the corresponding outcomes derived from the numerical analysis, refinements were made to the model parameters, facilitating its precise representation of the actual performance exhibited by the tunnel. This calibration process played a vital role in enhancing the reliability and predictive capabilities of the numerical model.

5. Finite Element Modeling

In the realm of contemporary engineering practices, numerical modeling has become indispensable for addressing complex phenomena [26]. Among the diverse array of numerical techniques available, the finite element method has emerged as a highly proficient tool for conducting simulations in geotechnical engineering [27].

5.1. Geometric Dimensions of the Model

The 2D numerical model employed in this study utilized a continuous field approach to accurately represent the twin tunnel and its surrounding soil layers. The geometric dimensions of the model were chosen in accordance with the prescribed German requirements outlined by Meissner [28].

To establish the bottom boundary of the model, Equation (2) was employed:

$$\mathrm{h} = (1.5 - 2.5) \times \mathrm{D} \tag{2}$$

where h represents the distance between the center point of the tunnel and the bottom boundary, and D corresponds to the diameter of the tunnel.

To determine the model width, Equation (3) was utilized:

$$\mathrm{w} = (4 - 5) \times \mathrm{D} \tag{3}$$

In this equation, w denotes the distance between the center point of the tunnel and the vertical boundaries.

The bottom of the model was fixed in both vertical and horizontal directions [Ux = Uy = 0], while the vertical boundaries were constrained horizontally [Ux = 0, Uy = free].

5.2. Material Model

To accurately simulate the behavior of the gravelly-sand soil encompassing the twin tunnels, both the HS (hardening soil) and HSS (hardening soil with small strain stiffness) models were employed, and the most appropriate model was selected. The water table was found to be situated at a depth of 15 m below the ground surface, and specific material properties of the gravelly-sand soil are presented in Table 1.

Table 1. The soil properties of the layers around the twin tunnel and the parameters of the material model.

(Hardening Soil Model: HS-Model, HS Small Model) (Gravelly Sand)		
Soil Parameters	**Symbol**	**Value**
Interface reduction factor	R_{inter} [−]	0.67
Overconsolidation ratio	OCR [−]	1
Exponential power	m [−]	0.4
Shear strain at 0.7 G_0	$\gamma_{0.7}$ [%]	0.0001
Small strain stiffness	G_0^{ref} [MPa]	250
Reference unloading–reloading stiffness	E_{ur}^{ref} [MPa]	144
Reference secant stiffness	E_{50}^{ref} [MPa]	48
Reference oedometer stiffness	E_{oed}^{ref} [MPa]	48
Unloading/reloading Poisson's ratio	v_{ur} [−]	0.2
Dilatancy angle	Ψ [°]	0
Cohesion	C' [kPa]	0
Internal friction angle	φ' [°]	33
Saturated unit weight	γ_{sat} [kN/m^3]	20

Regarding the twin tunnel lining, a beam element approach was utilized, featuring linear elastic behavior. To account for the influence of the joints between the precast concrete segments, a reduction factor of 4 was applied to the stiffness of the lining in curved sections. The use of this reduction factor, as recommended by Wood [29], aimed to ensure an accurate representation of the joint effects. Comprehensive details on the properties of the tunnel lining, including the reduction factors, are provided in Table 2.

Table 2. Properties of the tunnel lining.

Model	γ [kN/m^3]	EA [GN/m]	EI [MN.m^2]	v	t [cm]
Linear Elastic	25	10.5	19.69	0.15	30

5.3. Finite Element Mesh Analysis

This section provides a comprehensive investigation of the finite element method (FEM) mesh size utilized in the numerical modeling for the study. The primary significance of this analysis lies in its potential impact on the precision and reliability of the simulation results. Through a meticulous evaluation of the mesh size, the aim is to ensure that the numerical model can effectively capture the intricate behavior of the system under investigation.

To initiate the analysis, a diverse range of mesh sizes was selected to assess their influence on the simulation outcomes. A systematic variation of the mesh elements, with and without local refinement around the tunnel and ground surface, was performed to closely monitor any corresponding changes in the outcomes. This meticulous study aimed to carefully evaluate the trade-off between computational efficiency and solution accuracy, a crucial consideration in selecting an appropriate mesh size.

The investigation's findings, presented in Table 3 without local refinement, revealed that a coarse mesh size consisting of 164 elements led to minimal changes in maximum vertical settlements (Sv,max). Further increasing the number of elements did not significantly contribute to striking a favorable balance between computational efficiency and solution accuracy. Consequently, the decision was made to adopt a coarse mesh size, as it demonstrated a satisfactory compromise between computational efficiency and accuracy.

Table 3. The outcomes of the mesh sensitivity analysis conducted in the numerical model without local refinement.

Coarseness	Number of Elements	Sv,max (mm)
Very coarse	114	−11.2
Coarse	164	−11.53
Medium	324	−11.76
Fine	698	−11.89
Very fine	1466	−11.95

To better understand the impact of local refinement on enhancing results, a refinement factor of 0.25 was employed in critical regions adjacent to the ground surface and tunnels for various coarseness levels, addressing potential issues related to element distortion. As shown in Table 4, applying the coarse mesh with local refinement, using 703 elements, yielded minimal changes in maximum vertical settlements (Sv,max). Similarly, additional elements beyond this threshold did not significantly improve the balance between computational efficiency and solution accuracy, as depicted in Figure 2.

Table 4. The outcomes of the mesh sensitivity analysis conducted in the numerical model with local refinement.

Coarseness (with Local Refinement)	Number of Elements	Sv,max (mm)
Very coarse	471	−11.0753
Coarse	703	−11.4582
Medium	1463	−11.6834
Fine	2504	−11.8496

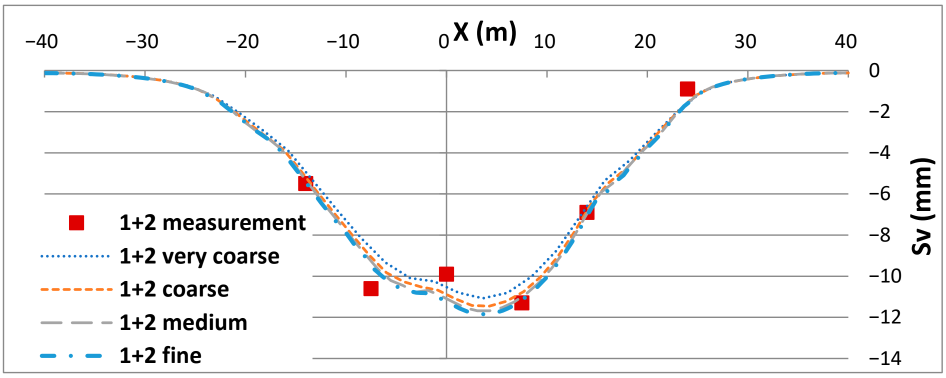

Figure 2. Transverse settlement trough of the two-dimensional model after excavation of twin tunnels (1 + 2) using HSS with different coarseness levels and local refinement around tunnels and ground surface (compiled by the authors based on [6]).

This strategic approach of mesh selection and refinement substantially improved the representation of the complex interaction between the soil, structures, and tunnel excavation. The chosen mesh density, combined with the application of local refinement using 703 elements (Figure 3), ensured that the simulation results closely aligned with the field measurements, as visually demonstrated in Figure 2. This meticulous approach in mesh selection and refinement resulted in simulation results that remained well within acceptable margins of deviation from the field measurements, reinforcing the robustness and reliability of our numerical model.

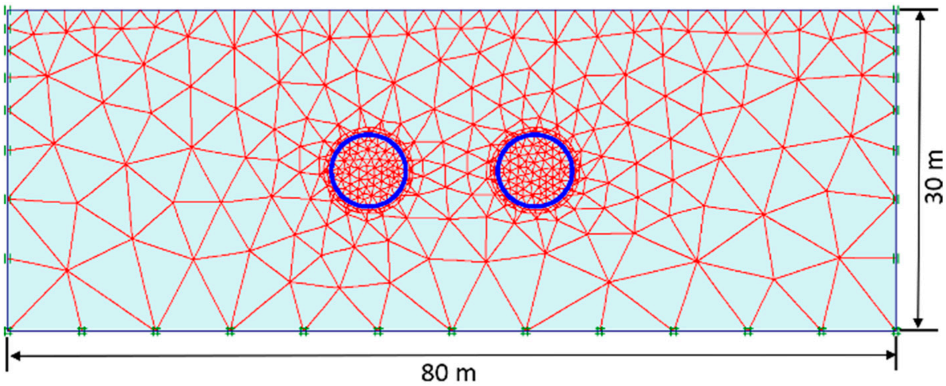

Figure 3. The mesh employed in the 2D numerical study.

Figure 3 provides a visual depiction of the geometric dimensions of the utilized model, with dimensions measuring 80 m in the x-direction and 30 m in the y-direction.

5.4. 2D Numerical Model

To validate the numerical modeling approach for simulating soil behavior during tunnel excavations, two constitutive models, namely HS (hardening soil) and HSS (hardening soil with small strain stiffness), were selected based on previous studies [6,7,23,30] that recommended their suitability. The numerical simulations were performed using a coarse mesh with local refinement, consisting of 703 elements. The validation process involved comparing the measured surface settlements obtained during the construction of a specific tunnel (reference field section S16) with the corresponding settlements calculated using numerical simulations.

Figure 4 illustrates a graphical portrayal of the vertical settlements observed in the soil consequent to the excavation of the first tunnel. Furthermore, Figure 5 presents a visual representation of the vertical settlements observed in the soil resulting from the excavation of the twin tunnel. Notably, it is evident that the settlements are predominantly concentrated above the position of the first tunnel. These graphical depictions allow for a clear understanding of the spatial distribution and concentration of settlements in relation to the tunnel excavation process.

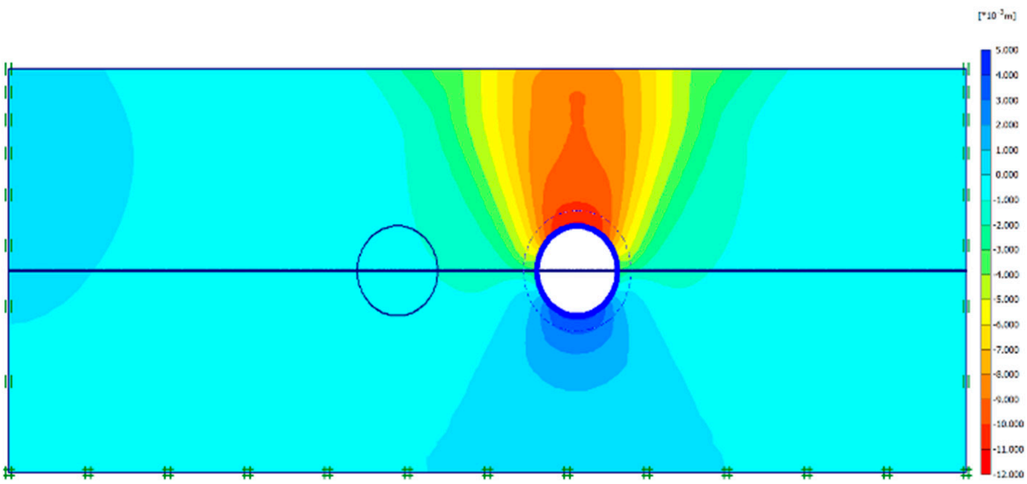

Figure 4. Resulting vertical settlements of soil using the method of contraction and (HSsmall) soil model after excavating the first tunnel.

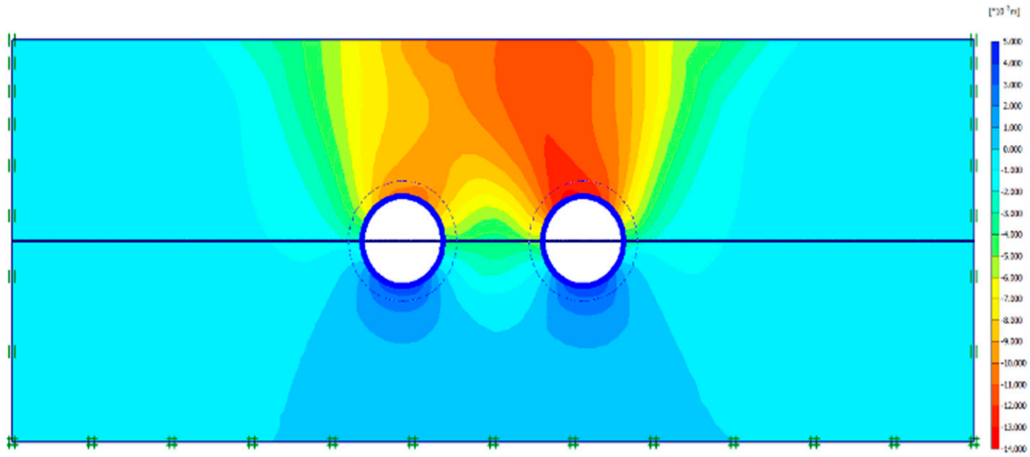

Figure 5. Resulting vertical settlements of soil using the contraction method and (HSsmall) soil model after the excavation of the two tunnels.

Figure 6 displays the transversal settlements measured in the field, as well as those calculated using the HS and HSS models for the excavation of the first tunnel (blue curves) and the twin tunnels (red curves). The results demonstrate that the HSS model yields a settlement trough that more closely aligns with the field measurements.

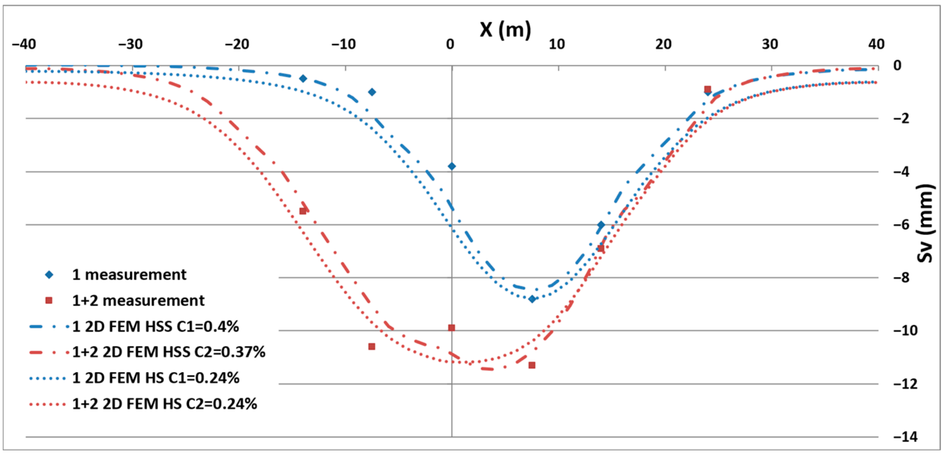

Figure 6. Transverse settlement trough of the two-dimensional model resulting from the excavation of the first tunnel and after the excavation of the twin tunnel using two different soil models (HS/HSS) (compiled by the authors based on [6]).

6. Results

To enhance understanding of the interaction between the soil, surface structure, and the excavation of twin tunnels, a comprehensive parametric study was conducted. This study aimed to investigate various influential parameters and their effects on the system. Additionally, a comparison was made between the conditions of a green field (GF) and the presence of a surface structure to isolate and clarify the individual effects of twin tunnel excavation and the presence of the structure. The parameters examined in this study are illustrated in Figure 7, while the characteristics of soil layers (1,2) can be found in Table 5. The structure was modeled using the equivalent beam method [7], with specific dimensions including a width of 13.5 m, foundation depth of 2 m, structure weight of 150 kPa, and a total of 10 stories.

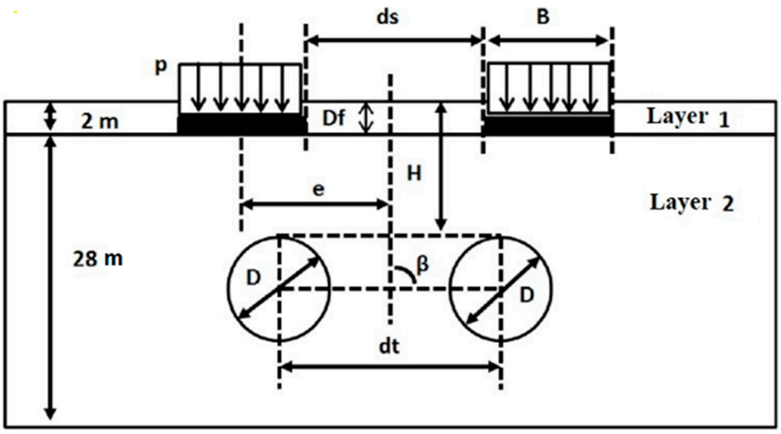

Figure 7. The examined parameters in the study.

Table 5. Properties of the soil layers used in the parametric study.

Soil Parameters	Symbol	Layer 1	Layer 2
Reference secant stiffness	E_{50}^{ref} [Mpa]	14	35
Reference oedometer stiffness	E_{oed}^{ref} [Mpa]	14	35
Reference unloading–reloading stiffness	E_{ur}^{ref} [Mpa]	42	105
Unloading/reloading Poisson's ratio	ν_{ur} [−]	0.2	0.2
Small strain stiffness	G_0^{ref} [Mpa]	52	175
Shear strain at 0.7 G_0	$\gamma_{0.7}$ [%]	0.0005	0.0005
Exponential power	m [−]	0.5	0.5
Overconsolidation ratio	OCR	1	1
Interface reduction factor	R_{inter}	0.67	0.67
Dilatancy angle	Ψ [°]	0	1
Cohesion	C' [kPa]	3	5
Internal friction angle	φ' [°]	27	35
Unsaturated unit weight	γ_{unsat} [kN/m^3]	17	20

In Figure 7, Df represents the foundation depth; P denotes the building load; ds signifies the spacing between symmetrical structures concerning the axis of the twin tunnels; dt indicates the distance between the axes of the twin tunnels; H represents the depth of the twin tunnels; D corresponds to the diameter of the twin tunnels; B stands for the building width; e is the distance between the axis of the twin tunnels and the axis of the structure; and β represents the angle between the vertical axis of the tunnels and the line connecting their centers.

Additionally, δ is used to denote the differential settlement between the edges of the building, while Sv,max represents the maximum vertical settlement experienced by the building. Furthermore, GF is employed as an abbreviation for green field, referring to the condition of an undeveloped site without any existing structures or facilities on the ground surface.

6.1. The Effect of Eccentricity (e)

The effect of eccentricity (e), defined as the distance between the axis of the twin tunnels and the axis of the structure, on the behavior of the system was investigated. The findings presented in Figure 8 provide insights into the relationship between eccentricity and various response parameters.

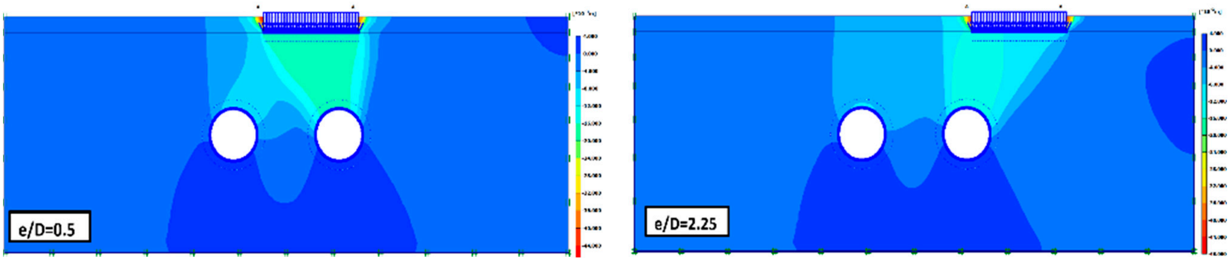

Figure 8. Contour map of displacements resulting from twin tunnel excavation at e/D = 0.5 and e/D = 2.25.

As eccentricity increases, it is observed that the effect of the twin tunnels on the structure decreases, as shown in Figure 9a. This can be attributed to the spatial separation between the tunnels and the structure, resulting in reduced direct interaction between them.

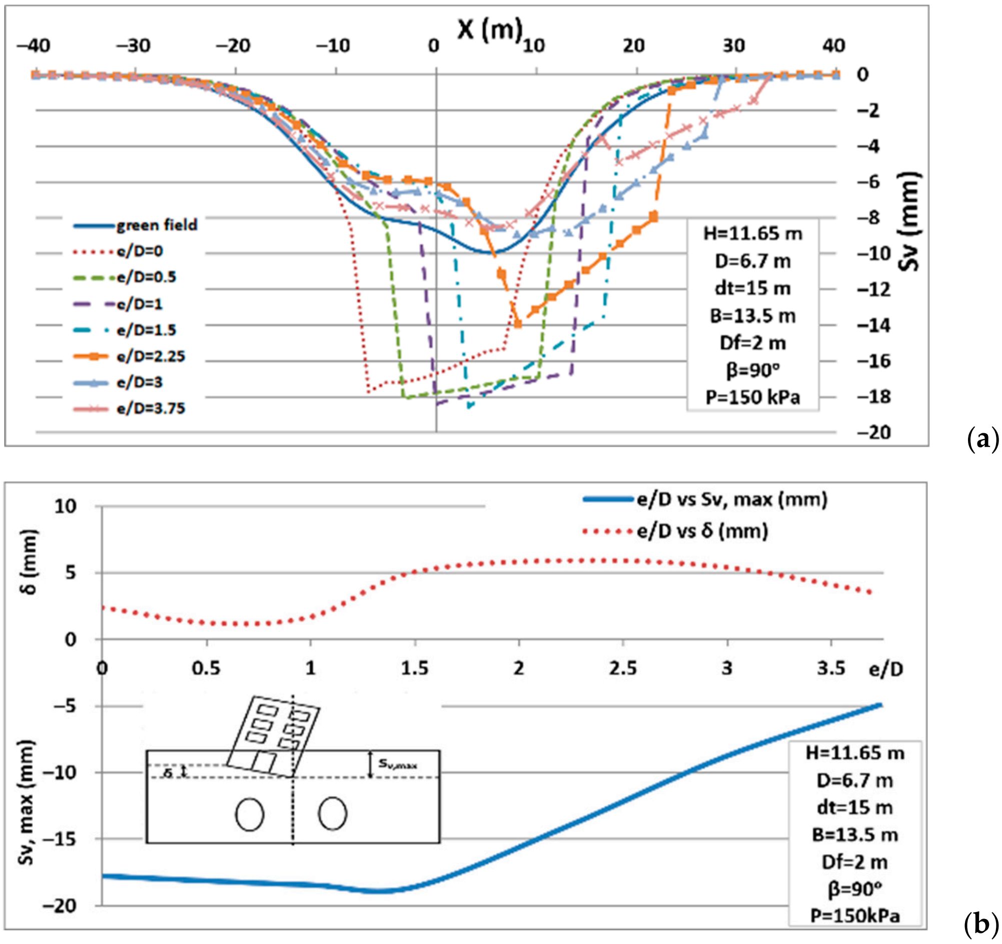

Figure 9. (**a**) Influence of eccentricity (e) on the transverse settlement trough. (**b**) Influence of eccentricity-to-diameter ratio (e/D) on maximum (Sv,max) and differential settlements (δ).

Regarding the structure itself, the maximum settlement (Sv,max) experiences a slight increase up to an eccentricity-to-diameter ratio of e/D = 1.5, as presented in Figure 9b. This can be attributed to the closer proximity of the structure to the tunnel, which results in a higher concentration of stress and deformation in that region. However, as the eccentricity surpasses this threshold, the settlement starts to decrease. Regarding the differential settlement (δ), a similar trend is observed as in the case of maximum settlement. Initially, there is an increase in the differential settlement until the eccentricity-to-diameter ratio reaches e/D = 1.5, indicating the occurrence of significant differential deformations within the structure. However, beyond this threshold, the differential settlement remains relatively constant for eccentricity values up to e/D = 3. Subsequently, after surpassing e/D = 3, the differential settlement starts to decrease, as depicted in Figure 9b.

6.2. The Effect of the Spacing (ds)

The investigation focused on studying the influence of the spacing (ds) between the two ends of symmetrical structures in relation to the axis of the twin tunnels. The results presented in Figure 10 provide valuable insights into the system's behavior as ds varies.

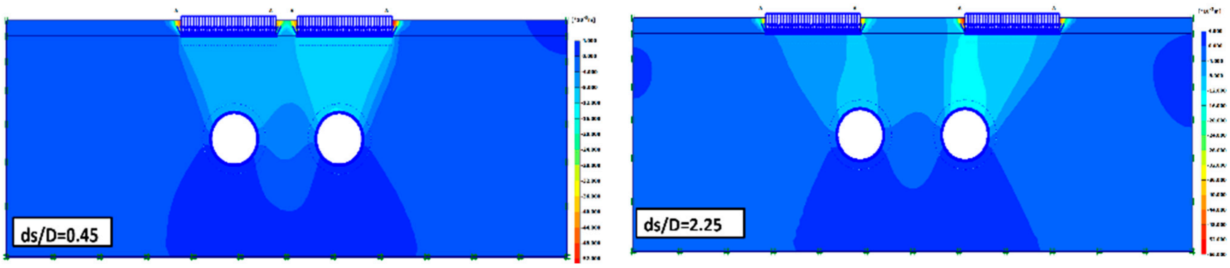

Figure 10. Contour map of displacements resulting from twin tunnel excavation at ds/D = 0.45 and ds/D = 2.25.

For small values of ds, there is a joint action between the two structures and the twin tunnels. However, as the distance between the two structures increases, this mutual action diminishes, and each structure becomes predominantly influenced by the tunnel located directly beneath it, as shown in Figure 11a. Consequently, increasing the spacing between the two structures leads to a decrease in overall mutual action.

The spacing between the structures has a significant impact on the subsidence and settlement trough resulting from the excavation of the twin tunnels. As the distance between the two structures increases, the subsidence decreases, and the resulting settlement trough widens, as illustrated in Figure 11a. This can be attributed to the reduced interaction between the twin tunnels and the structures, resulting in less concentrated deformation effects.

Regarding the structures themselves, a decrease in the maximum settlement is observed starting from a spacing-to-diameter ratio of ds/D = 1.4, as shown in Figure 11b. This decrease can be attributed to the reduced influence of the twin tunnels and the increased spatial separation between the structures. On the other hand, an increase in the differential settlement is observed with an increase in the distance between the two structures until ds/D = 1.4. Beyond this point, the changes in the differential settlement become slight, indicating a diminished effect, as presented in Figure 11a.

These findings highlight the significance of the spacing between the two structures in understanding the mutual action between the structures and the twin tunnels. Increasing the spacing reduces the mutual action and allows for more independent behavior of each structure with respect to the tunnel beneath it. The decrease in subsidence, widening of the settlement trough, decrease in the maximum settlement, and changes in the differential settlement are all influenced by the distance between the two structures.

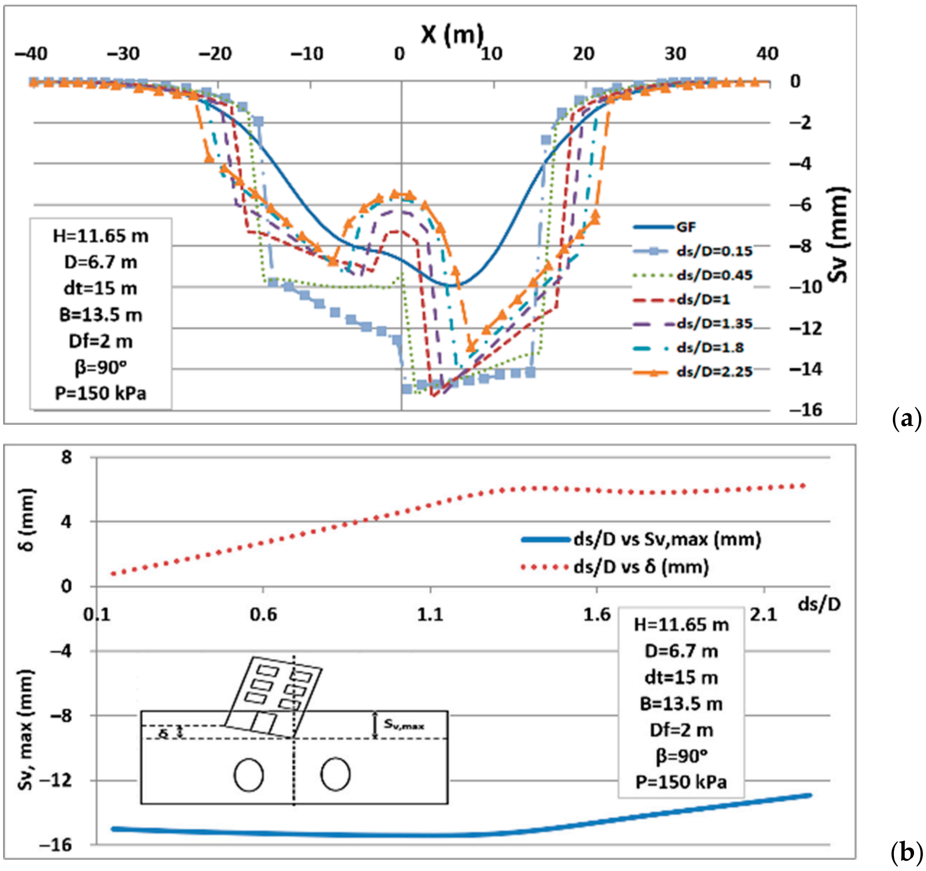

Figure 11. (**a**) Influence of the spacing (ds) between the two ends of symmetrical structures on the transverse settlement trough. (**b**) Influence of spacing-to-diameter ratio (ds/D) on maximum (Sv,max) and differential settlements (δ).

6.3. The Effect of the Depth of the Twin Tunnels (H)

The impact of the depth of the twin tunnels (H) on the system's behavior was examined to understand its influence on the interaction between the tunnels and the surrounding soil. The results, illustrated in Figure 12, provide valuable insights into the relationship between H and different deformation patterns.

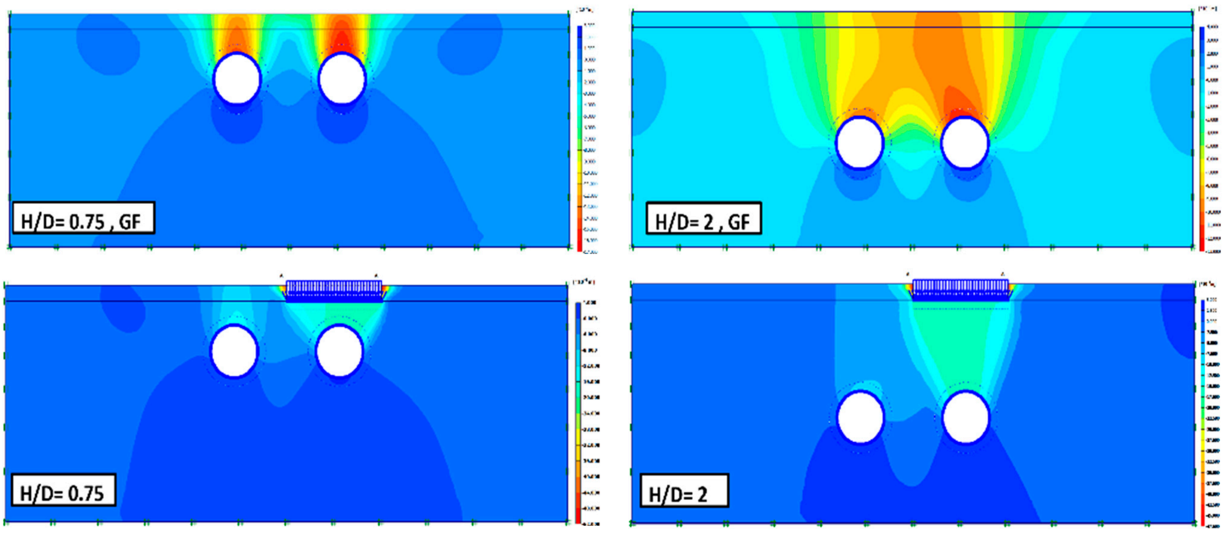

Figure 12. Contour map of displacements resulting from twin tunnel excavation at H/D = 0.75 and H/D = 2.

As the soil thickness above the twin tunnels decreases, whether in the absence of existing structures or with the presence of the original structure, the interaction effect between the twin tunnels diminishes. This is particularly evident starting from a depth-to-diameter ratio of H/D = 1.25, as depicted in Figure 13a,b. At this point, the deformations resulting from the twin tunnels begin to separate.

In the case of the green field (GF) condition, the subsidence trough undergoes a distinct separation into two troughs positioned at the top of each twin tunnel. However, in the presence of a structure, the behavior changes due to its interaction with the twin tunnels. The maximum settlement of the structure initially occurs towards the axis of the two tunnels and then shifts towards the axis of the tunnel located below the structure as it approaches the surface, as shown in Figure 13a,b, which illustrates the relationship between twin tunnel depth and settlements. It was observed that as the depth of the twin tunnels increased, the maximum settlements and differential settlements exhibited a decreasing trend up to a depth-to-diameter ratio of H/D = 1.25. This indicates that deeper tunnels resulted in reduced settlements and differential settlements in the surrounding soil and structures. Beyond the depth-to-diameter ratio of H/D = 1.25, the maximum settlements and differential settlements showed a slight change, suggesting a relatively stable behavior.

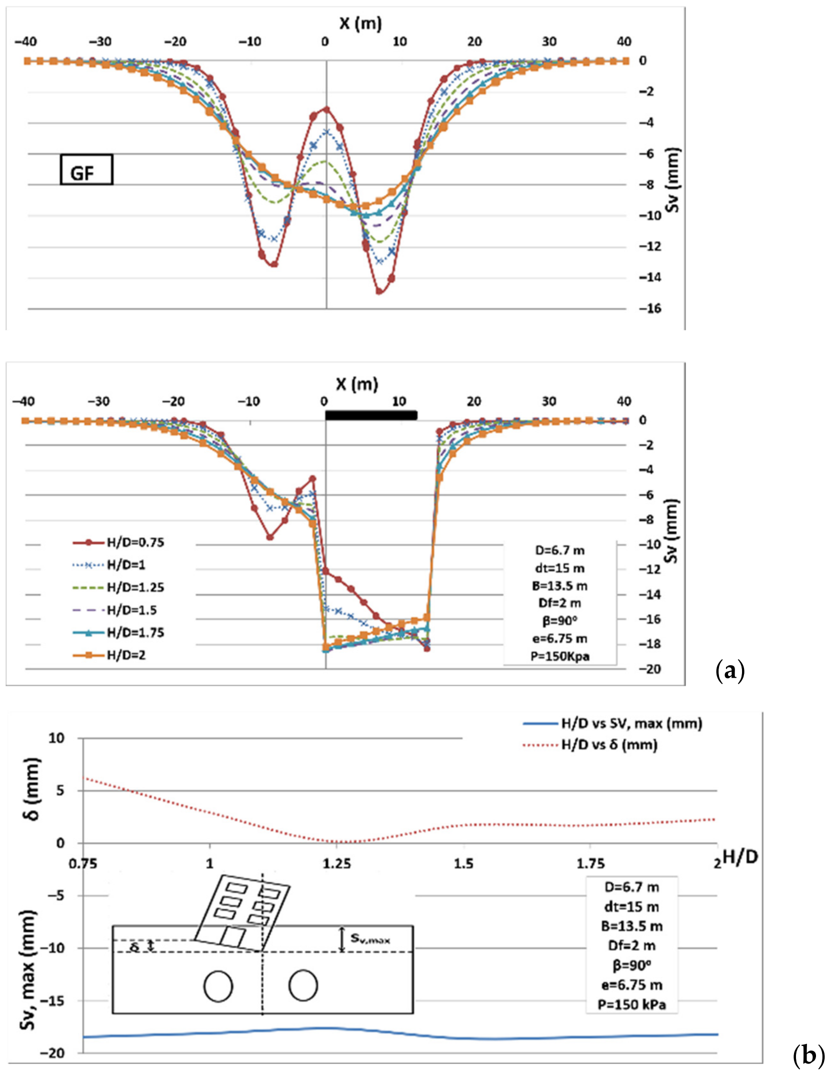

Figure 13. (**a**) Influence of depth of the twin tunnels (H) on the transverse settlement trough. (**b**) Influence of (H/D) on maximum (Sv,max) and differential settlements (δ).

These observations indicate that the depth of the twin tunnels significantly influences the interaction effects and deformation patterns. Decreasing the soil thickness above the tunnels leads to a reduction in the interaction between the tunnels and the surrounding soil, resulting in more separated deformations. The distinct separation of subsidence troughs in the green field condition and the rotation of the structure's settlement towards the axis of the twin tunnels and then towards the axis of the lower tunnel highlight the intricate nature of the interaction phenomenon.

6.4. The Effect of the Diameter of the Twin Tunnels (D)

The investigation revealed that the thickness of the soil above the twin tunnels, as considered in this analysis, is adequate to induce interaction between the tunnels, irrespective of their diameter, under both green field conditions and in the presence of a structure (Figure 14). The findings demonstrate a clear correlation between the diameter of the twin tunnels and the extent of subsidence and the size of the subsidence trough.

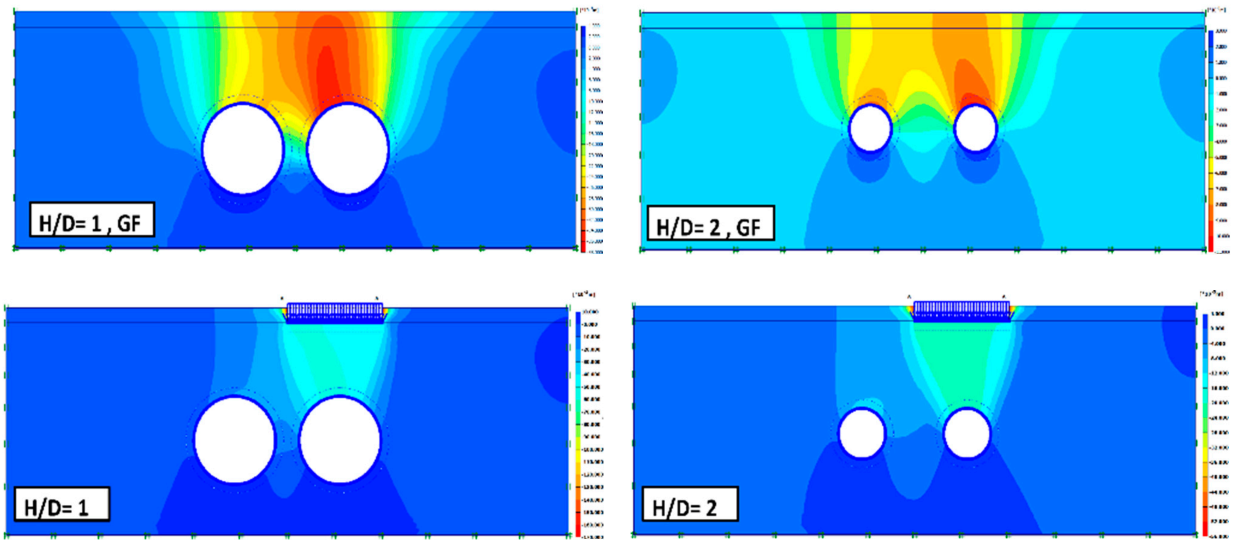

Figure 14. Contour map of displacements resulting from twin tunnel excavation at H/D = 1 and H/D = 2.

In the case of the green field (GF), as well as with the presence of the structure, an increase in the diameter of the twin tunnels leads to elevated levels of subsidence and a larger subsidence trough as illustrated in Figure 15a. This behavior can be attributed to the heightened deformations resulting from the excavation of larger tunnels. The considerable influence of tunnel diameter on the settlement response necessitates careful consideration during the design and construction of structures near twin tunnels of varying diameters.

Regarding the structure itself, the study revealed that the maximum settlement decreases with an increase in the ratio of the depth of the tunnels to their diameter (H/D). This relationship suggests that as the ratio of H/D increases, the maximum settlement experienced by the structure decreases. However, the changes in the differential settlement between the two ends of the structure were found to be minimal, indicating that the effect of tunnel diameter on this parameter is relatively insignificant as shown in Figure 15b.

6.5. The Effect of the Distance between the Axis of the Twin Tunnels (dt)

The study investigated the effect of the distance between the axes of the twin tunnels (dt) on the system behavior, particularly the interaction between the tunnels and the surrounding soil. The results, illustrated in Figure 16, provide valuable insights into the relationship between dt and different deformation patterns. The results provide detailed insights into this relationship.

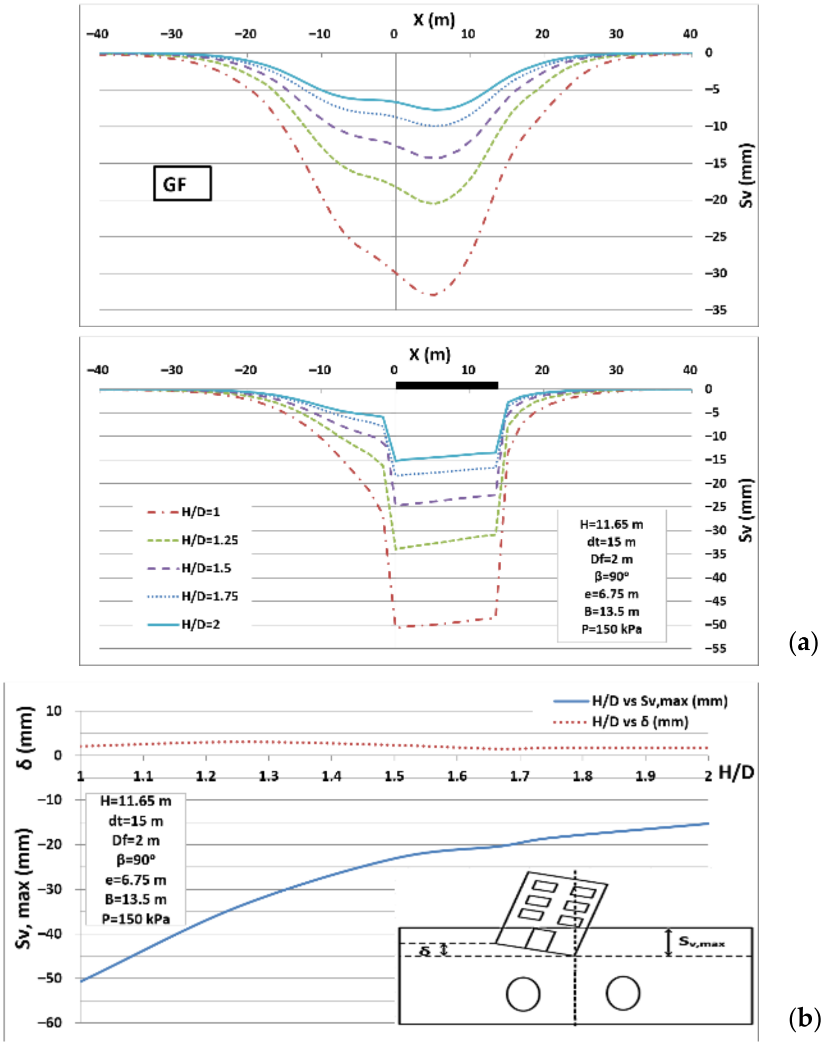

Figure 15. (**a**) Influence of the diameter of the twin tunnels (D) on the transverse settlement trough. (**b**) Influence of (H/D) on maximum (Sv,max) and differential settlements (δ).

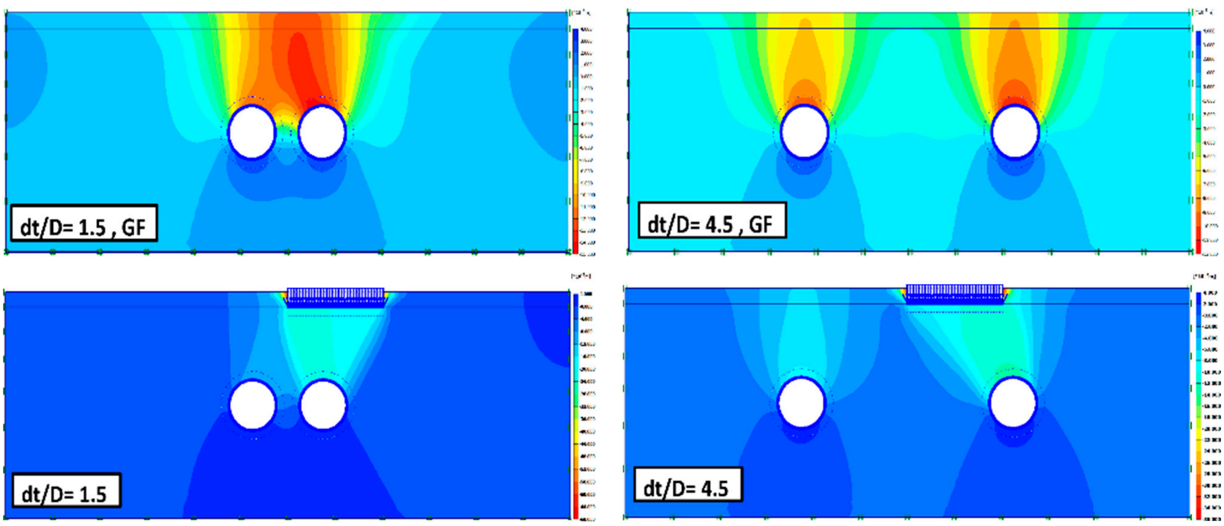

Figure 16. Contour map of displacements resulting from twin tunnel excavation at dt/D = 1.5 and dt/D = 4.5.

1- Decreased interaction effect: As the distance between the tunnel axes (dt) increases, the interaction effect between the twin tunnels decreases. This means that the tunnels' influence on each other diminishes, and they behave more independently. This is evident in the formation of separate subsidence troughs for each tunnel as illustrated in Figures 16 and 17a.
2- Separate subsidence troughs: In the case of the green field (GF), where no structure is present, the separate subsidence troughs become more pronounced as dt/D increases. This indicates that each tunnel operates individually, and their excavations have minimal impact on one another as shown in Figure 17a.
3- Rotation change in the presence of a structure: When a structure is present above the tunnels, its behavior changes with respect to the tunnel axes as presented in Figure 17a. Initially, the structure aligns with the axis of the twin tunnels. However, as dt increases, the structure's rotation shifts, and it aligns more with the axis of the tunnel located below the structure. This rotation change signifies the altered interaction dynamics between the structure and the twin tunnels.
4- Specific case of dt/D = 3: When the distance between the tunnel axes (dt) reaches a value of three times the tunnel diameter (D), the tunnels operate separately, even in the presence of a structure. This is particularly evident in the case of the green field, where the separation of the subsidence troughs is more pronounced as illustrated in Figure 17b.

The obtained results provide valuable insights into the system behavior and the influence of varying the distance between the tunnel axes. This knowledge is of utmost importance for the design and construction of twin tunnels, as it ensures their stability and helps mitigate potential risks associated with tunneling operations.

6.6. The Effect of Placing the Two Tunnels in Relation to Their Axis (β)

The influence of the positioning of twin tunnels in relation to their axis (β) was investigated to examine its effect on system behavior. β represents the angle between the vertical axis of the tunnels and the line connecting their centers, with a positive direction from the plumb, clockwise.

The results demonstrate distinct patterns of interaction between the twin tunnels when considering both the green field condition and the presence of a structure. The strongest interaction occurs when the tunnels are positioned adjacent to each other or on top of each other, resulting in the intersection of collapse surfaces generated during excavation. However, if one tunnel is situated higher than the other, the upper tunnel exerts a dominant influence on the subsidence trough as shown in Figure 18.

In the case of the green field, the maximum subsidence is observed when the tunnels are placed on top of each other (β = 0). This is followed by the first tunnel being on top (β = 45), and then the second tunnel being on top (β = 135). The least subsidence occurs when the two tunnels are placed adjacent to each other (β = 90) as illustrated in Figure 19.

When a structure is present, the most critical scenario is when the tunnels are positioned on top of each other (β = 0), followed by the first tunnel being on top (β = 45), and when the tunnels are placed adjacent to each other (β = 90). The least subsidence occurs when the second tunnel is excavated on top and positioned far from the structure (β = 135) as shown in Figure 19. By carefully considering the positioning of the tunnels with respect to their axis, engineers can mitigate subsidence effects and minimize potential hazards associated with tunneling activities.

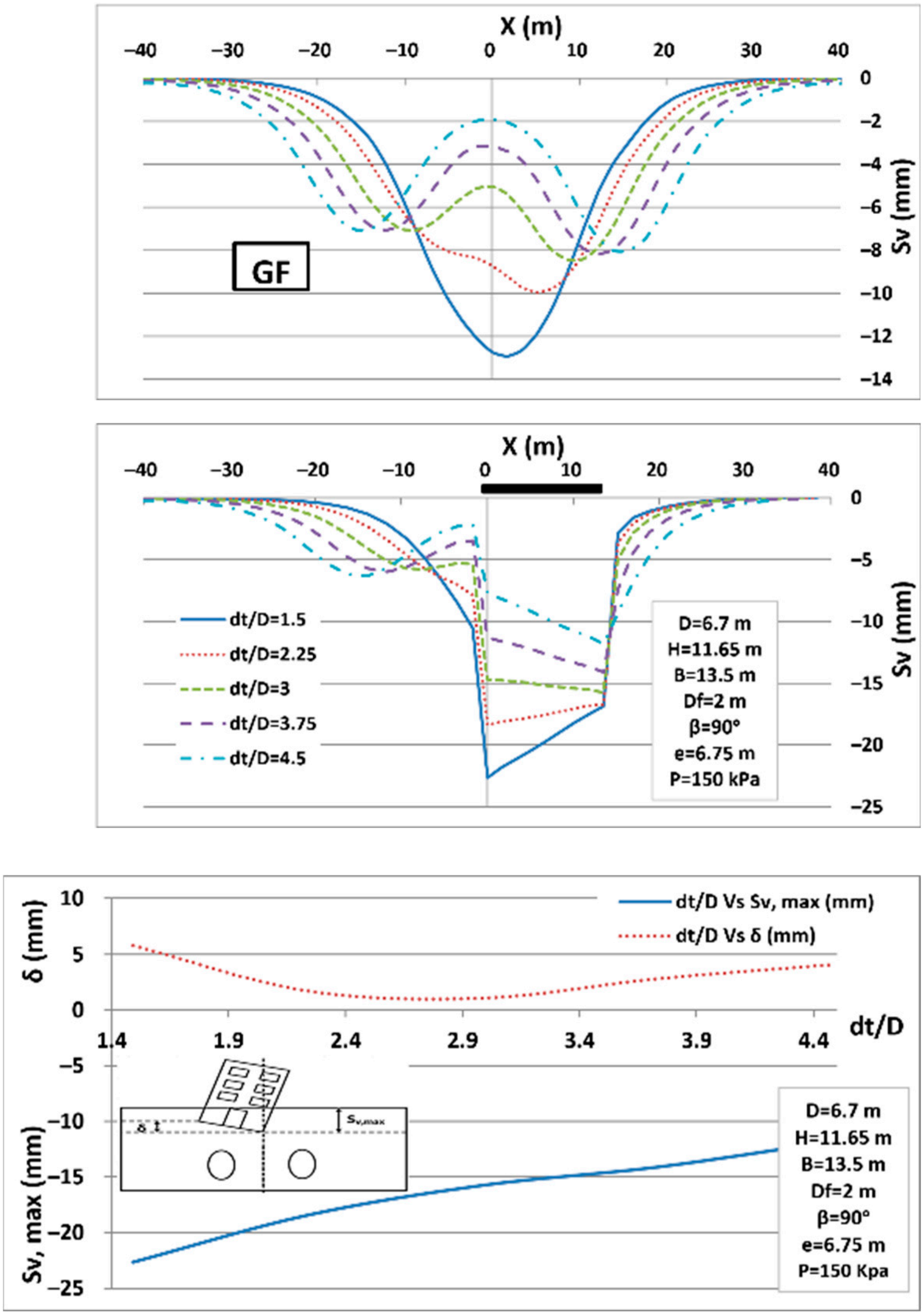

(**a**)

(**b**)

Figure 17. (**a**) Influence of the distance between the axis of the twin tunnels (dt) on the transverse settlement trough. (**b**) Influence of (dt/D) on maximum (Sv,max) and differential settlements (δ).

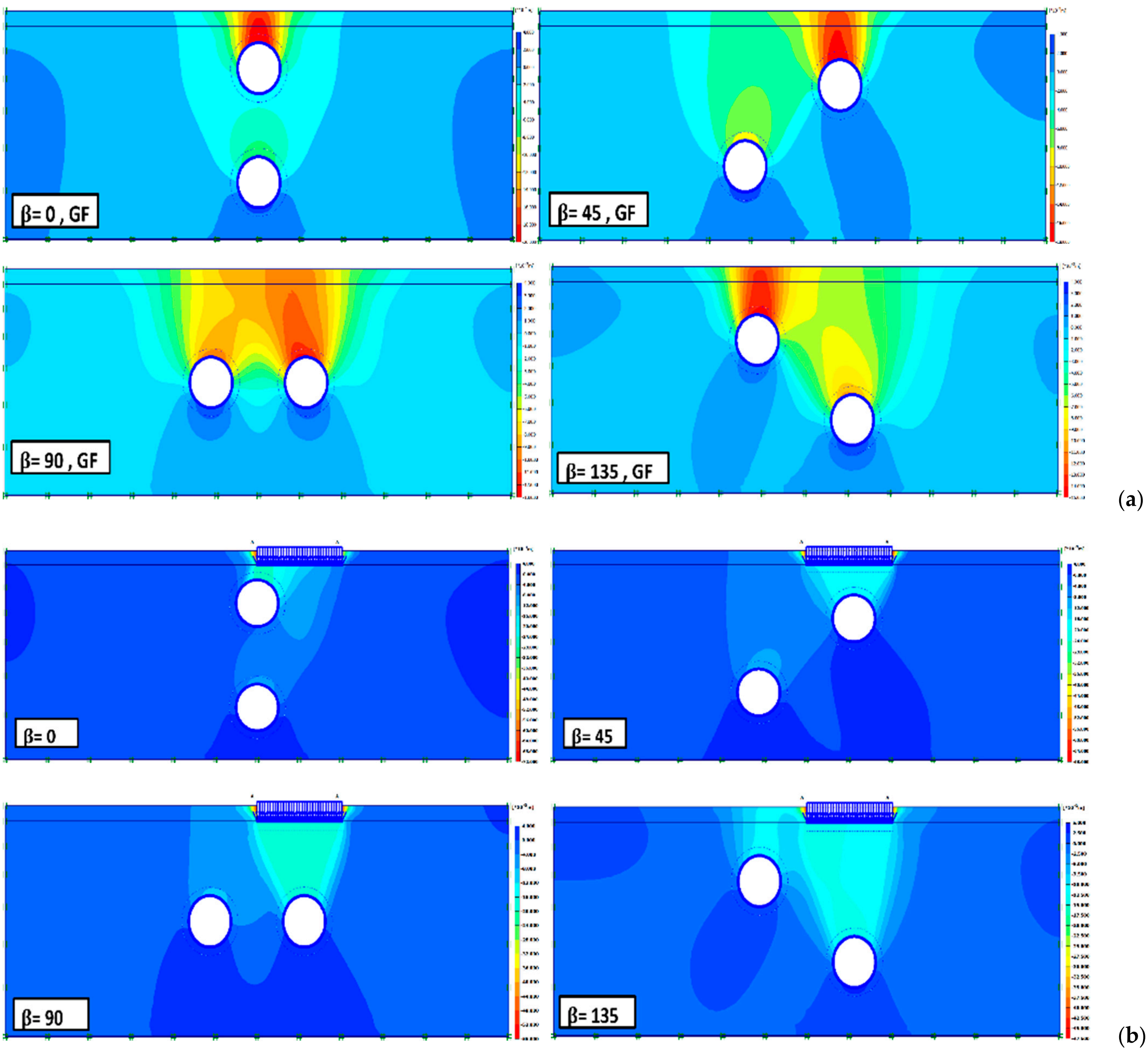

Figure 18. Contour map of displacements resulting from twin tunnel excavation at different β values (**a**) in the case of the green field (**b**) when a structure is present.

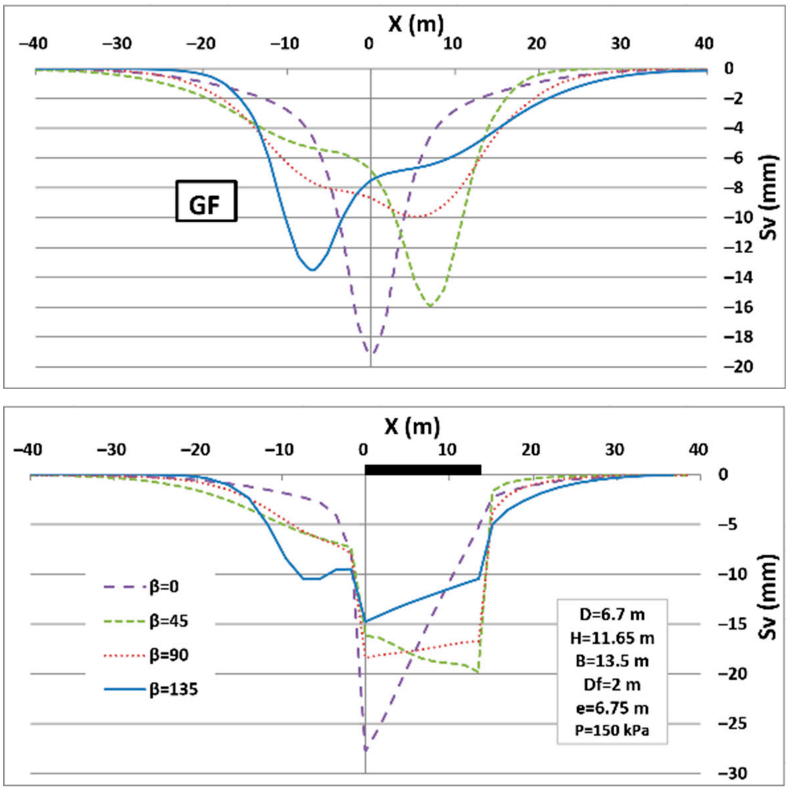

Figure 19. Influence of placing the two tunnels in relation to their axis (β) on the transverse settlement trough.

7. Conclusions

In this study, a comprehensive analysis of various parameters influencing the interaction between soil-surface structure and twin tunnel excavation was conducted. The numerical analysis was supported by a calibration process to ensure the accuracy and reliability of the simulation results.

The calibration process involved adjusting and validating the finite element method (FEM) model used in the study. This was achieved by comparing its predictions with well-established reference field measurements obtained from the renowned Milan Tunnel in Italy. The calibration process allowed us to anchor the model's predictions to real-world behavior and provided confidence in the accuracy of the numerical simulations. As a result of the calibration process, the HSS and coarse mesh size with local refinement around the tunnel and ground surface were determined to provide the best results.

Subsequently, with a calibrated model, the study investigated the impact of various parameters on twin tunnel behavior and their influence on the surrounding soil and structures. The results of the analysis led to the following conclusions:

1- Eccentricity (e): The maximum settlement experiences a slight increase up to an eccentricity-to-diameter ratio (e/D) of 1.5. Beyond this ratio, the influence of eccentricity on settlement becomes less significant.
2- Spacing (ds): A decrease in the maximum settlement is observed starting from a spacing-to-diameter ratio (ds/D) of 1.4. This indicates that increasing the distance between the two ends of symmetrical structures in relation to the axis of the twin tunnels reduces the interaction effect between them.
3- Depth of twin tunnels (H): As the soil thickness above the twin tunnels decreases, either in the absence of existing structures or with the presence of the original structure, the interaction effect between the tunnels diminishes. This effect becomes prominent starting from a depth-to-diameter (H/D) ratio of 1.25.

4- Diameter of twin tunnels (D): Increasing the diameter of the twin tunnels leads to elevated levels of subsidence and a larger subsidence trough in both the green field scenario and with the presence of a structure.
5- Distance between tunnel axes (dt): When the distance between the tunnel axes (dt) reaches a value of three times the tunnel diameter (D), the tunnels operate separately, even in the presence of a structure. This indicates that the spacing between the tunnels plays a critical role in their independent behavior.
6- Tunnel positioning (β): The results reveal distinct patterns of interaction between twin tunnels. Placing the tunnels adjacent to each other or on top of each other results in the greatest interaction, where collapse surfaces from excavation intersect. However, when one tunnel is positioned higher than the other, the upper tunnel dominates the subsidence trough.

The calibration process, along with the comprehensive analysis, enhances the understanding of the complex phenomena associated with twin tunnels and their interaction with the surrounding soil and structures. The findings of this study enhance the understanding of the complex phenomena associated with twin tunnels and their interaction with the surrounding soil and structures. These insights enable engineers to make informed decisions during the design and construction phases, leading to the implementation of appropriate design strategies and risk mitigation measures. However, it is essential for future research to explore the effects of the longitudinal direction using advanced 3D simulation approaches to gain a more comprehensive understanding of twin tunnel interactions and to account for the limitations of 2D simulations.

Author Contributions: Conceptualization, A.A., A.S., R.R. and H.A.; investigation, A.A.; Methodology, A.A. and A.S.; writing—original draft preparation, A.A.; numerical modeling, A.S., A.A., R.R. and H.A.; Validation, A.A. and A.S.; writing—review and editing, A.A., A.S., R.R. and H.A. All authors have read and agreed to the published version of the manuscript.

Funding: This research received no external funding.

Data Availability Statement: Data will be made available upon request.

Conflicts of Interest: The authors declare no conflict of interest.

Nomenclature

R_{inter}	Interface reduction factor [−]
OCR	Overconsolidation ratio [−]
m	Exponential power [−]
$\gamma_{0.7}$	Shear strain at 0.7 G_0 [%]
G_0^{ref}	Small strain stiffness [MPa]
E_{ur}^{ref}	Reference unloading–reloading stiffness [MPa]
E_{50}^{ref}	Reference secant stiffness [MPa]
E_{oed}^{ref}	Reference oedometer stiffness [MPa]
ν^{ur}	Unloading/reloading Poisson's ratio [−]
C'	Cohesion [kPa]
φ'	Internal friction angle [°]
Ψ	Dilatancy angle [°]
γ	Unit weight [kN/m^3]
γ_{unsat}	Unsaturated unit weight [kN/m^3]
γ_{sat}	Saturated unit weight [kN/m^3]
EA	Normal stiffness [GN/m]
EI	Bending stiffness [MN.m^2]
t	Lining thickness [cm]
ν	Poisson's ratio [−]
h	The distance between the center point of the tunnel and the bottom boundary [m]
w	The distance between the center point of the tunnel and the vertical boundaries [m]
D	Diameter of the tunnel [m]

B	Building width [m]
e	The distance between the axis of the twin tunnels and the axis of the structure [m]
ds	The spacing between the two ends of symmetrical structures [m]
H	The depth of the twin tunnels [m]
β	The angle between the vertical axis of the tunnels and the line connecting their centers, with a positive direction from the plumb, clockwise [°]
Sv,max	Maximum vertical settlements [mm]
δ	The differential settlement between the edges of the building [mm]
GF	Green field
FEM	Finite element method
TBM	Tunnel boring machine

References

1. Gong, C.; Ding, W.; Xie, D. Twin EPB tunneling-induced deformation and assessment of a historical masonry building on Shanghai soft clay. *Tunn. Undergr. Space Technol.* **2020**, *98*, 103300. [CrossRef]
2. Kaczmarek, Ł.; Popielski, P. Numerical Analysis of the Impact of Construction of an Underground Metro Line on the Urban Environment: A Case Study from the Vistula Valley in Warsaw. *Przegląd Geol.* **2016**, *64*, 219–229.
3. Peng, F.; Ma, S.; Li, M.; Fu, K. Stress Performance Evaluation of Shield Machine Cutter Head during Cutting Piles under Masonry Structures. *Adv. Civ. Eng.* **2022**, *2022*, 4111637. [CrossRef]
4. Mathew, G.V.; Lehane, B.M. Measured and Back Analysed Soil Structure Interaction Effects in a Layered Stratigraphy During Tunnel Boring. *Geotech. Geol. Eng.* **2014**, *32*, 873–884. [CrossRef]
5. Hao, D.; Zhu, R.; Wu, K.; Chen, R. Analysis of Ground Settlement Caused by Double-line TBM Tunnelling Under Existing Building. *Geotech. Geol. Eng.* **2022**, *40*, 899–911. [CrossRef]
6. Fargnoli, V.; Boldini, D.; Amorosi, A. Twin tunnel excavation in coarse grained soils: Observations and numerical back-predictions under free field conditions and in presence of a surface structure. *Tunn. Undergr. Space Technol.* **2015**, *49*, 454–469. [CrossRef]
7. Maleki, M.; Sereshteh, H.; Mousivand, M.; Bayat, M. An equivalent beam model for the analysis of tunnel-building interaction. *Tunn. Undergr. Space Technol.* **2011**, *26*, 524–533. [CrossRef]
8. Katebi, H.; Rezaei, A.; Hajialilue-Bonab, M.; Tarifard, A. Assessment the influence of ground stratification, tunnel and surface buildings specifications on shield tunnel lining loads (by FEM). *Tunn. Undergr. Space Technol.* **2015**, *49*, 67–78. [CrossRef]
9. Giardina, G.; DeJong, M.J.; Mair, R.J. Interaction between surface structures and tunnelling in sand: Centrifuge and computational modelling. *Tunn. Undergr. Space Technol.* **2015**, *50*, 465–478. [CrossRef]
10. Farrell, R.P. Tunnelling in Sands and the Response of Buildings. Ph.D. Thesis, University of Cambridge, Cambridge, UK, 2011.
11. Son, M. Response analysis of nearby structures to tunneling-induced ground movements in sandy soils. *Tunn. Undergr. Space Technol.* **2015**, *48*, 156–169. [CrossRef]
12. Son, M. Response analysis of nearby structures to tunneling-induced ground movements in clay soils. *Tunn. Undergr. Space Technol.* **2016**, *56*, 90–104. [CrossRef]
13. Boldini, D.; Losacco, N.; Bertolin, S.; Amorosi, A. Finite Element modelling of tunnelling-induced displacements on framed structures. *Tunn. Undergr. Space Technol.* **2018**, *80*, 222–231. [CrossRef]
14. Mroueh, H.; Shahrour, I. A full 3-D finite element analysis of tunneling–adjacent structures interaction. *Comput. Geotech.* **2003**, *30*, 245–253. [CrossRef]
15. Mirhabibi, A.; Soroush, A. Effects of surface buildings on twin tunnelling-induced ground settlements. *Tunn. Undergr. Space Technol.* **2012**, *29*, 40–51. [CrossRef]
16. Duangsano, O.; Yensri, P.; Chayaroon, A.; Timpong, S.; Jongpradist, P. Tunnelling impacts and mitigation on existing structures for Bangkok MRT Orange Line. *Géoméch. Tunn.* **2023**, *16*, 272–280. [CrossRef]
17. Sarfarazi, V.; Asgari, K. Influence of Single Tunnel and Twin Tunnel on Collapse Pattern and Maximum Ground Movement. *J. Min. Environ.* **2022**, *13*, 117–128. [CrossRef]
18. Li, S.; Li, P.; Zhang, M.; Liu, Y. Influence of Approaching Excavation on Adjacent Segments for Twin Tunnels. *Appl. Sci.* **2019**, *10*, 98. [CrossRef]
19. Khan, Z.A.; Sadique, M.R.; Samanta, M. Evaluation of Surface Settlement Due to Construction of Twin Transportation Tunnels in Soils. *Transp. Infrastruct. Geotechnol.* **2023**, 1–22. [CrossRef]
20. Chortis, F.; Kavvadas, M. Three-Dimensional Numerical Investigation of the Interaction Between Twin Tunnels. *Geotech. Geol. Eng.* **2021**, *39*, 5559–5585. [CrossRef]
21. Cavalcanti, M.D.; Nahas Ribeiro, W.; Cabral dos Santos Junior, M. Engineering Challenges for Safe and Sustainable Underground Occupation. *Infrastructures* **2023**, *8*, 42. [CrossRef]
22. Zucca, M.; Valente, M. On the limitations of decoupled approach for the seismic behaviour evaluation of shallow multi-propped underground structures embedded in granular soils. *Eng. Struct.* **2020**, *211*, 110497. [CrossRef]
23. Alsirawan, R.; Sheble, A.; Alnmr, A. Two-Dimensional Numerical Analysis for TBM Tunneling-Induced Structure Settlement: A Proposed Modeling Method and Parametric Study. *Infrastructures* **2023**, *8*, 88. [CrossRef]
24. Vermeer, P.A.; Brinkgreve, R. *Plaxis Version 5 Manual*; AA Balkema: Rotterdam, The Netherlands, 1993.

25. Govindasamy, D.; Ismail, M.A.M.; Zaki, M.F.M.; Ken, T.Y.; Cheah, F.; Likitlersuang, S. Assessment of the Twin-Tunnel Interaction Mechanism in Kenny Hill Formation Using Contraction Ratio Method. *Indian Geotech. J.* **2020**, *50*, 825–837. [CrossRef]
26. Alsirawan, R.; Alnmr, A. Dynamic behavior of gravity segmental retaining walls. *Pollack Period.* **2022**, *18*, 94–99. [CrossRef]
27. Chen, Q. *An Experimental Study on Characteristics and Behavior of Reinforced Soil Foundation*; Louisiana State University and Agricultural and Mechanical College: Baton Rouge, LA, USA, 2007.
28. Meißner, H. Tunnelbau Unter Tage-Empfehlungen Des Arbeitskreises. *Numer. Geotech. EANG* **1996**, *19*, 99–108.
29. Muir Wood, A.M. The Circular Tunnel in Elastic Ground. *Géotechnique* **2015**, *25*, 115–127. [CrossRef]
30. Alnmr, A. Material Models to Study the Effect of Fines in Sandy Soils Based on Experimental and Numerical Results. *Acta Tech. Jaurinensis* **2021**, *14*, 651–680. [CrossRef]